U.S. NAVAL RESEARCH LABORATORY

OFFICE OF NAVAL RESEARCH

Sensitivity and Predictability of Mesoscale Polar Lows

James D. Doyle[1] and Kevin Biernat[2]

[1]U.S. Naval Research Laboratory, Monterey, CA
[2]National Research Council, Monterey, CA

We acknowledge the support of the Office of Naval Research Arctic Cyclone DRI and the U.S. Naval Research Laboratory Base Program.
Computational support provided by the Navy DoD Supercomputing Resource Center

What are Polar Lows?

- Small, intense cyclones with short horizontal scales and limited lifetimes
- Form within, or at the leading edge of a cold air mass moving over warmer sea surfaces in high latitudes (Shapiro et al. 1987)
- Associated with strong surface winds and heavy precipitation, posing hazards to ships and infrastructure (Businger and Reed 1989)
- May be spawned by high-latitude PV maxima or Tropopause Polar Vortices (TPVs) (Pyle et al. 2004; Cavallo and Hakim 2009; Kolstad 2011)
- In spite of NWP advances, the prediction of polar lows remains a challenge
  - ➢ Polar lows may be difficult to predict because of small scales and the role of diabatic processes (fluxes and convection) (Moreno-Ibáñez et al. 2021)
  - ➢ Mesoscale-synoptic-scale errors can grow rapidly and limit predictability (Lorenz 1969; Durran et al. 2013; Lloveras et al. 2023)

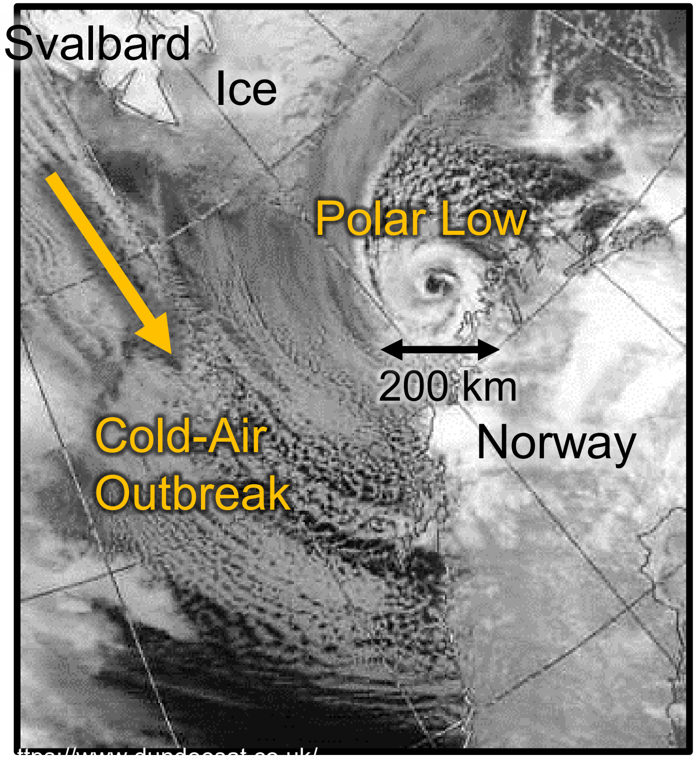

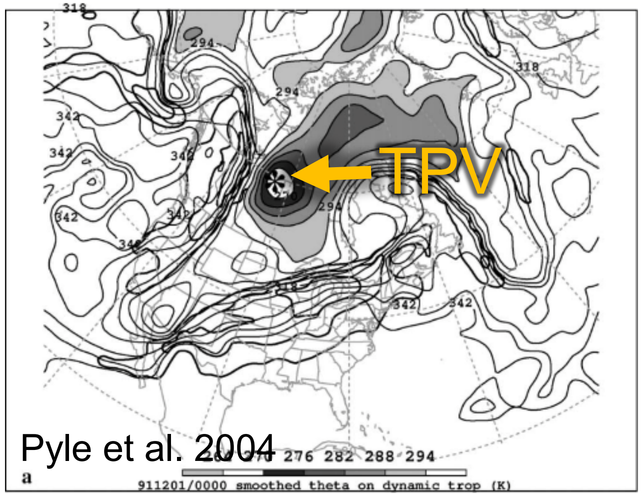

- What are the mesoscale initial state sensitivity “seeds” for polar low genesis?
- What are the sensitivity and predictability characteristics of polar lows?
- To what degree are polar lows spawned by TPVs?

COAMPS Model and Adjoint

- 36-h simulation initialized at 06 UTC 10 Feb. 2011 using 9-km coarse & 3-km fine mesh
    - Simulations also initialized at 00 UTC 10 Feb. 2011 and 12 UTC 10 Feb. 2011
- GFS at 1° horizontal resolution for initial and 6-hourly boundary conditions
- Parameterizations
    - Bulk, single moment microphysics (Rutledge and Hobbs 1983; Lin et al. 1983).
    - Longwave and shortwave radiation: Fu-Liou Scheme (Fu and Liou 1992, 1993).
    - 1.5 order turbulent kinetic energy closure PBL scheme (Mellor and Yamada 1982).

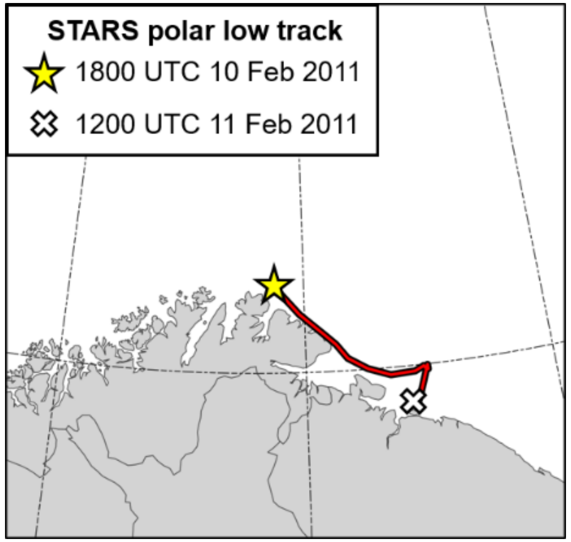

Characterize stability of system by examining the behavior of perturbation growth in linear framework

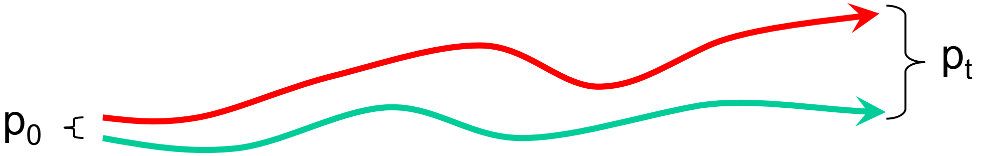

Nonlinear

$$p_t = Mx_0 - M(x_0 + p_0)$$

Nonlinear Model — State vector — Perturbation vector

Tangent Linear

$$p_t = M_{0,t}\, p_0$$

Tangent forward propagator or Tangent Linear Model (TLM)

Adjoint

$$\frac{\partial J}{\partial \mathbf{x}(t_0)} = \mathbf{M}^T \frac{\partial J}{\partial \mathbf{x}(t_n)}$$

Sensitivity of response function (J) at time t_n to the state at time t_0

- Adjoint allows for the quantification of the sensitivity of a forecast metric (pressure and PV) to changes in initial state
- Adjoint optimal perturbations allow us to see how small, but structured initial perturbations, impact the forecast
- COAMPS adjoint includes a suite of moist physics (microphysics, TKE PBL…) (9-km resolution)

Polar Lows and TPVs

- 140 polar lows occurred during 2002–2011 from the Sea Surface Temperature and Altimeter Synergy for Improved Forecasting of Polar lows dataset (STARS-DAT) archive (Sætra et al. 2010; https://projects.met.no/stars/).
- Polar lows dataset compared with a TPVs dataset constructed using ERA-Interim (Dee et al. 2011) and a TPV tracking algorithm (Szapiro and Cavallo 2018) to identify polar lows linked to TPVs.
- Determined which polar lows may be linked to TPVs by requiring that a polar low is located within 500 km of at least one TPV during the lifetime of the polar low.
- Selected a representative case, 10–11 Feb. 2011, to explore the processes, sensitivity and predictability.

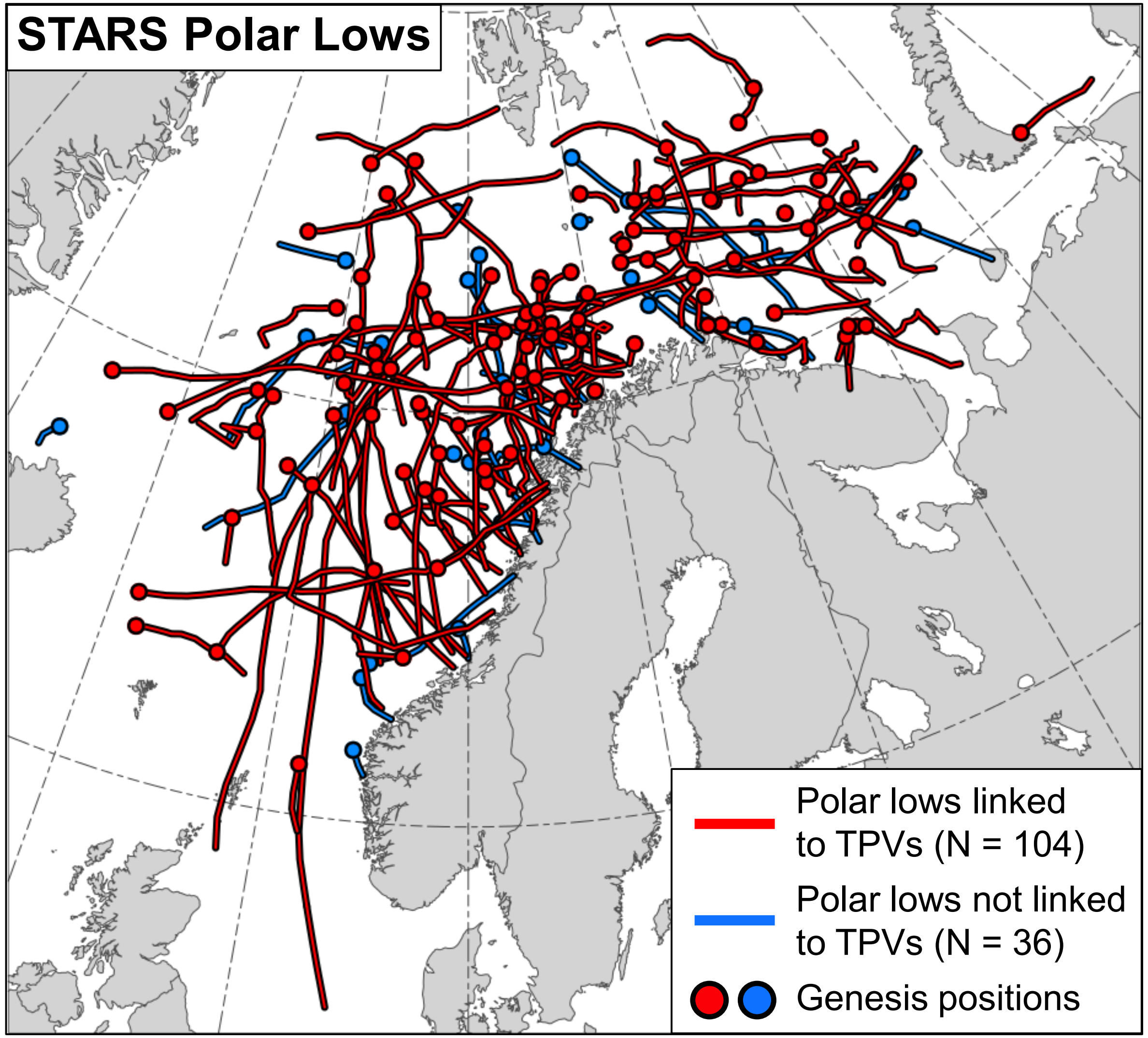

104 out of the total 140 polar lows, or 74%, match with at least one TPV

Synoptic-Scale Overview

- 9-km coarse mesh grid initialized at 06 UTC 10 Feb.
- Cold air outbreak conditions over the Barents Sea with large surface fluxes
- Northerly 300-hPa jet passes over Svalbard
- TPV was moving SSE of Svalbard

300-hPa winds (m s^{-1}; shading), 1000–500-hPa Thickness (blue), MSLP (hPa; black)

0600 UTC 10 Feb 2011 (F000) | **1800 UTC 10 Feb 2011 (F012)** | **0600 UTC 11 Feb 2011 (F024)**

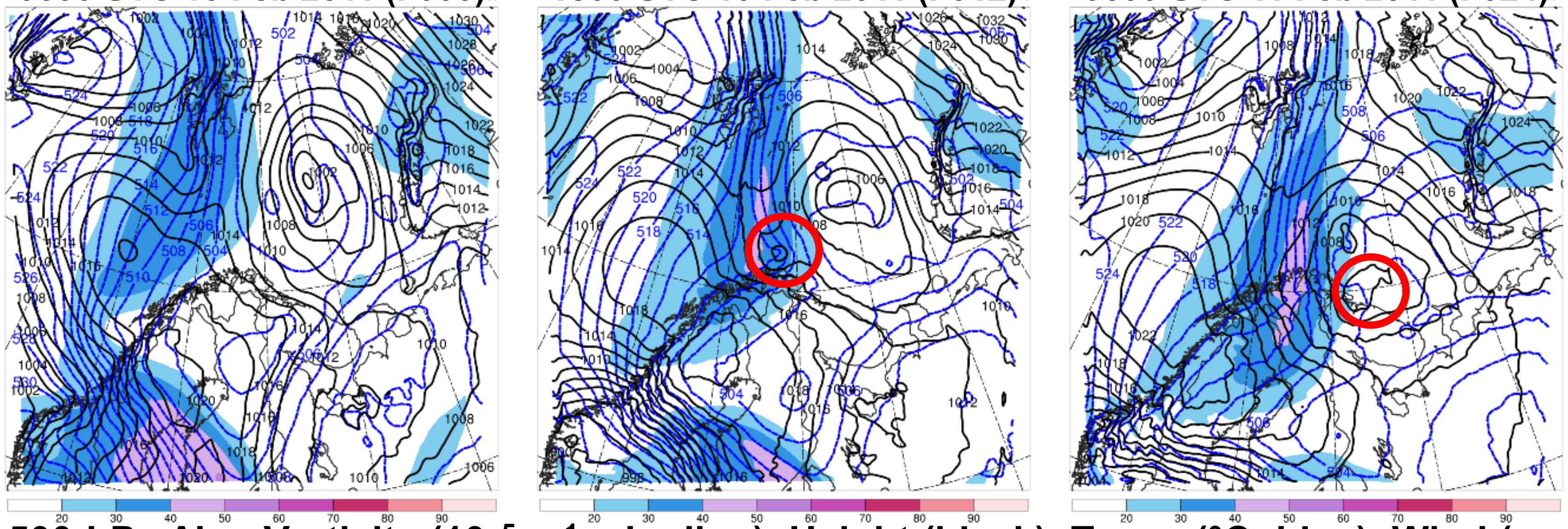

500-hPa Abs. Vorticity (10^{-5} s^{-1}; shading), Height (black), Temp. (°C; blue), Wind (m s^{-1})

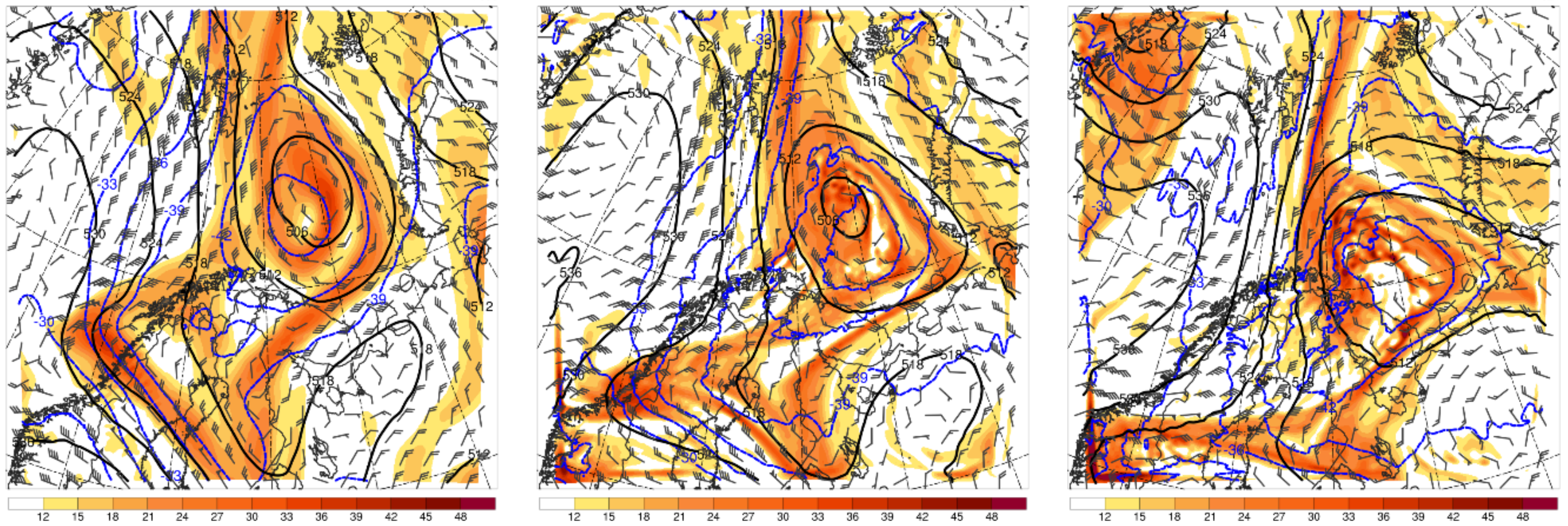

Mesoscale Overview

	0600 UTC 10 Feb. (0h)	1200 UTC 10 Feb. (06h)	1800 UTC 10 Feb. (12h)	0000 UTC 11 Feb. (18h)

10-m wind speed ($m\ s^{-1}$; shading), winds ($m\ s^{-1}$), MSLP (hPa; black)

850-hPa abs. vort. ($10^{-5}\ s^{-1}$; shading), height (black), temperature (°C; blue), wind (ms^{-1})

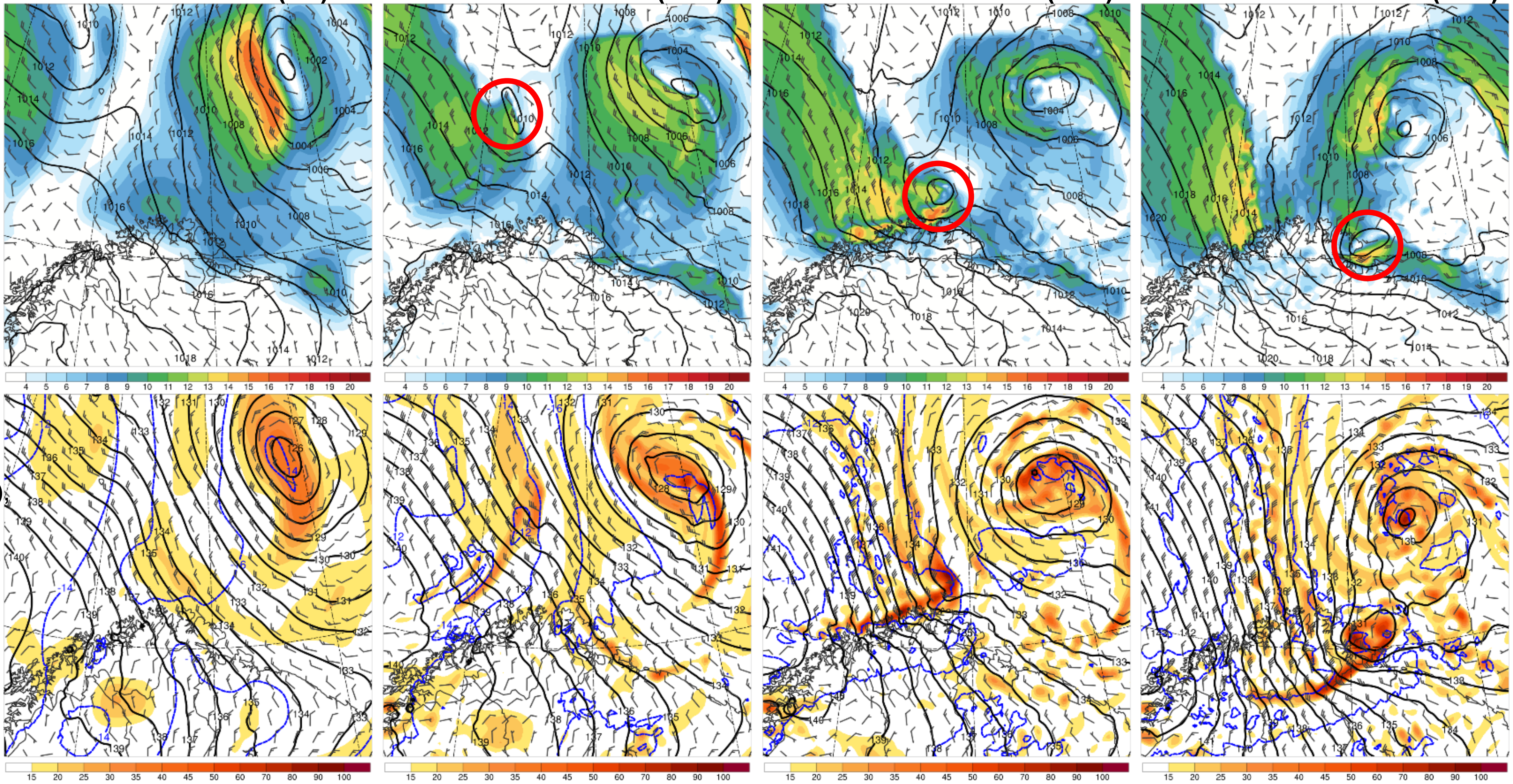

Polar low intensifies along a shallow baroclinic zone with strong shear vorticity

Verification and Sensitivity to Initialization Time

U.S. NAVAL RESEARCH LABORATORY

COAMPS nest 2 (3 km) fields valid at 1900 UTC 10 Feb 2011

10-m wind speed (m s^{-1}; shading) and wind (m s^{-1}; flags and barbs), and MSLP (hPa; black)

Initialized 0000 UTC 10 Feb (F019)

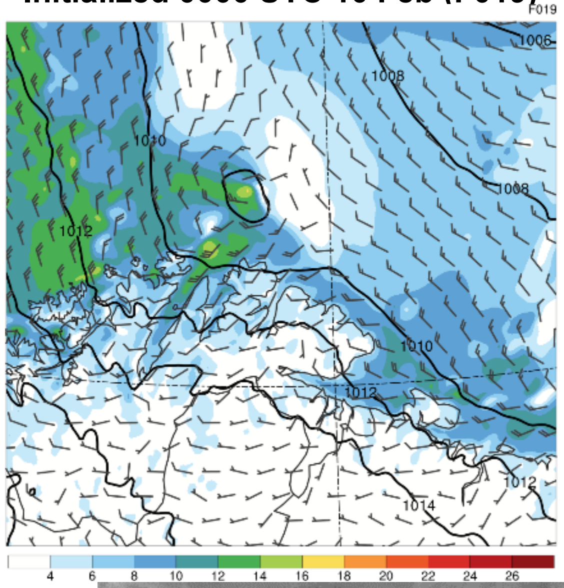

Initialized 0600 UTC 10 Feb (F013)

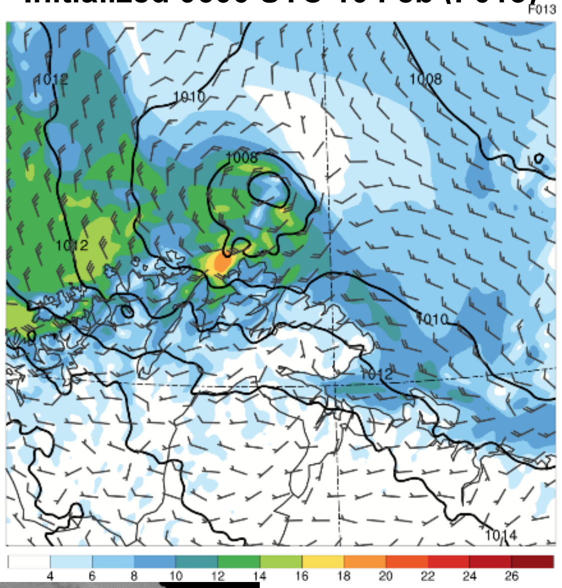

Initialized 1200 UTC 10 Feb (F007)

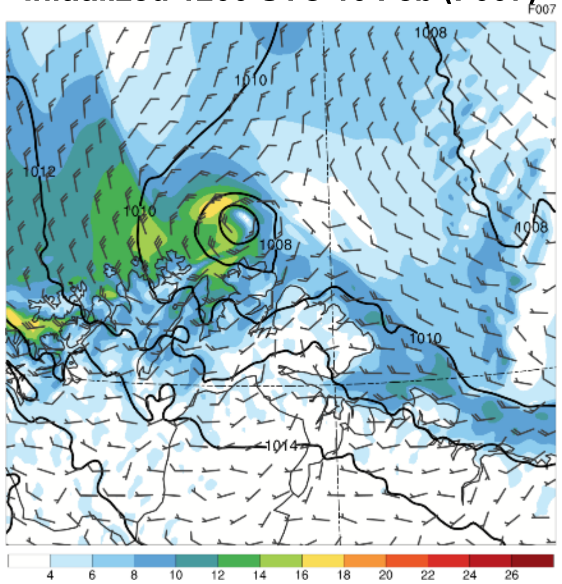

Envisat ASAR wind speed (m s^{-1}) valid at 1912 UTC 10 Feb 2011

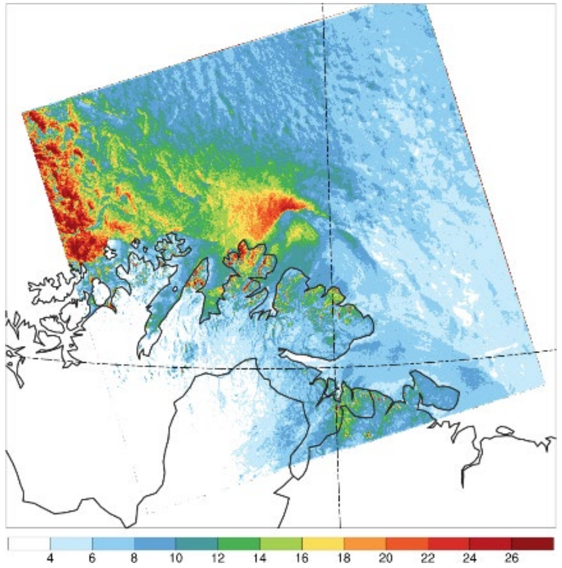

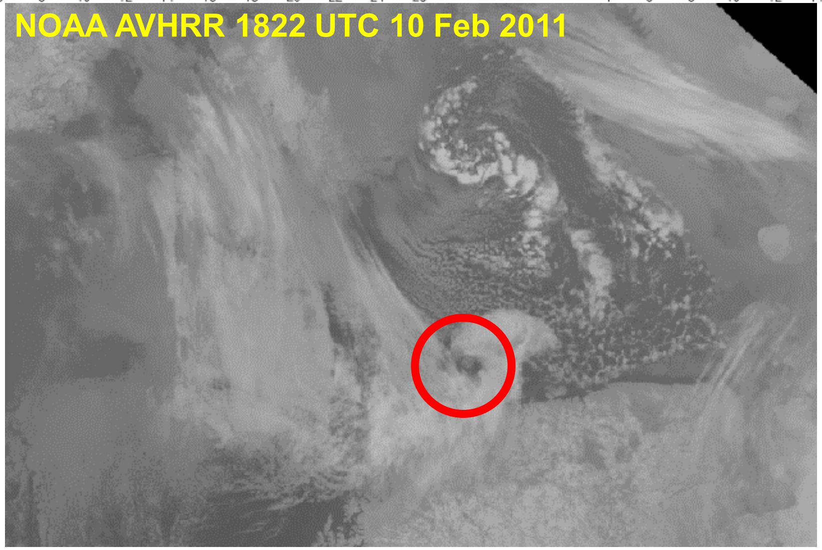

- Even the 3-km resolution mesh fails to significantly intensify polar low relative to the ASAR observations.
- Sensitivity of the polar low wind field and intensity to the initialization time.

NOAA AVHRR satellite imagery and Envisat advanced synthetic aperture radar (ASAR) wind speed data obtained from STARS-DAT archive (https://projects.met.no/stars/data/v3/).

Polar Low Intensity Adjoint Sensitivity

COAMPS (9 km) 12-h Forecast Sensitivity Valid at 0600 UTC 10 Feb 2011

850-hPa q (g kg^{-1}; shading), winds (arrows), q sensitivity (red/blue)

850-hPa abs. vorticity (x10^{-5} s^{-1}; shading), heights (black), rel. vorticity sensitivity (red/blue)

Surface latent heat flux (W m^{-2}; shading), 10-m, winds (arrows), LH flux sensitivity (red/blue)

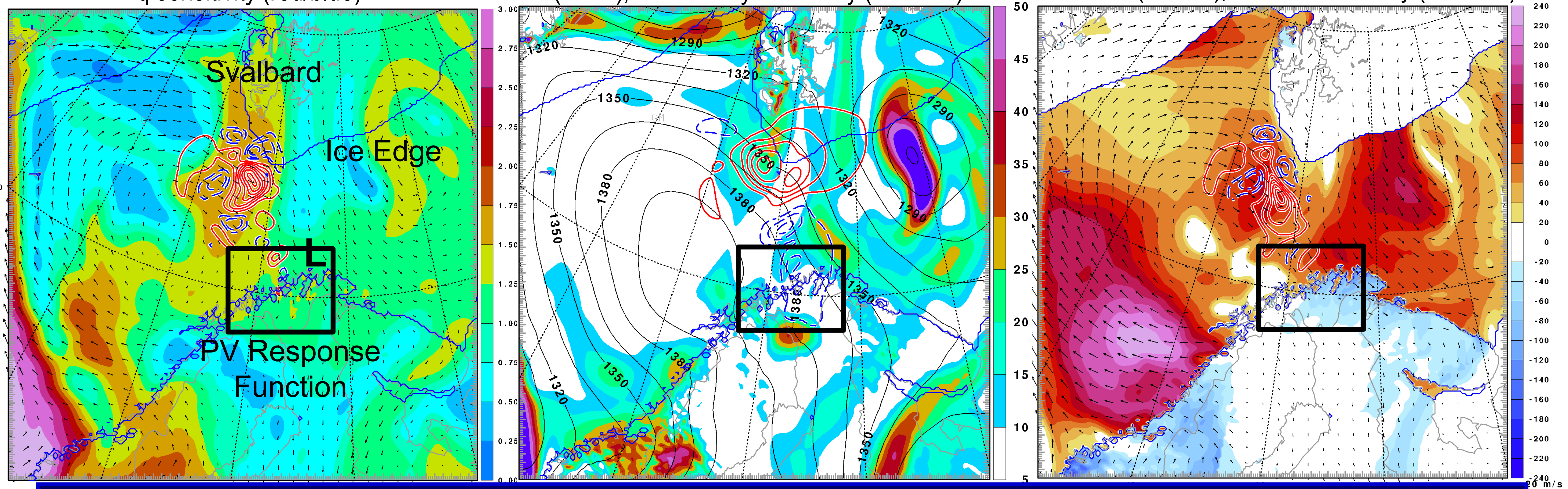

- PV response function is the 925-800 hPa PV over the forecast polar low at 12-h
- Strong sensitivities are in the low levels (850-hPa and below) and weaker sensitivities to the TPV
- 12-h forecast PV associated with the polar low intensification is sensitive to:
  - Low-level water vapor plume near ice edge (↑ 0-h water vapor ➡ ↑ 12-h PV in the polar low)
  - Low-level vorticity near ice edge in the NW flow (↑ 0-h vorticity ➡ ↑ 12-h PV in the polar low)
  - Surface latent heat flux south of ice edge (↑ 0-h surface latent heat flux ➡ ↑ 12-h PV in the polar low)

Polar Low Adjoint Optimal Perturbations

COAMPS (9 km) 12-h Forecast and Optimal Perturbations Valid at 1800 UTC 10 Feb 2011

925-hPa PV (PVU; shading), winds (arrows), heights (black); PV optimal pert. (1 PVU; red/blue)

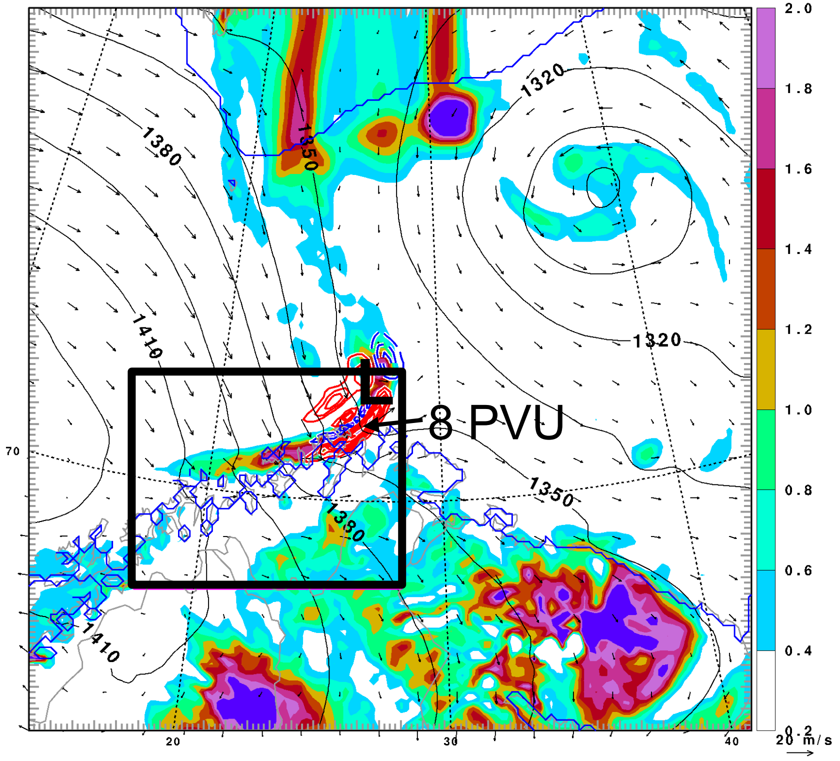

925-hPa wind speed (m s^{-1}; shading, arrows), SLP, wind speed optimal pert. (3 m s^{-1}; red/blue)

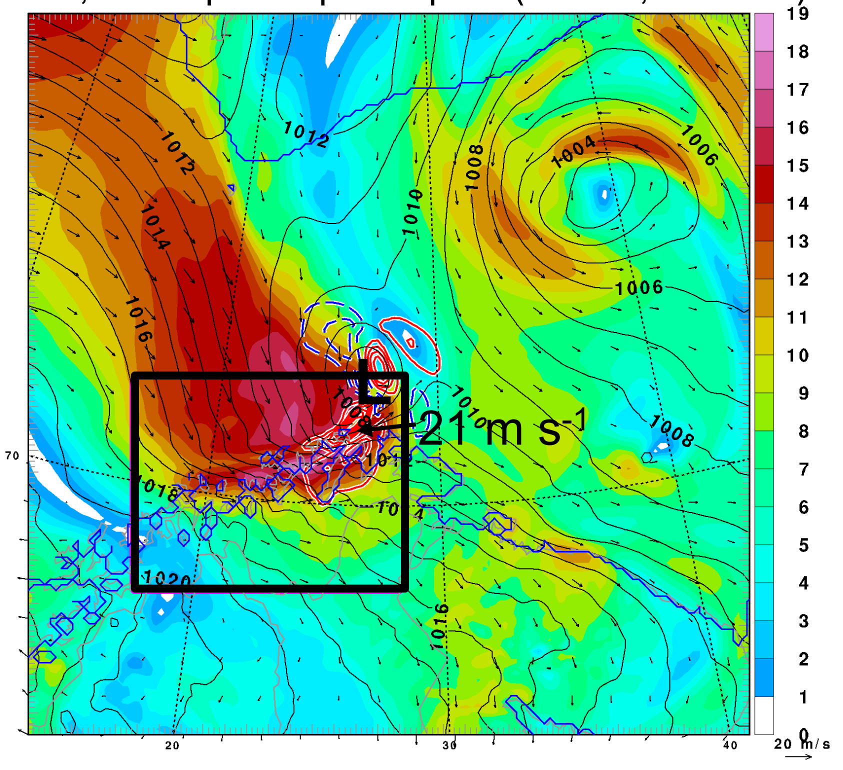

925-hPa diabatic heating (°C h^{-1}; shading), winds, diabatic heating optimal pert. (°C h^{-1}; red/blue)

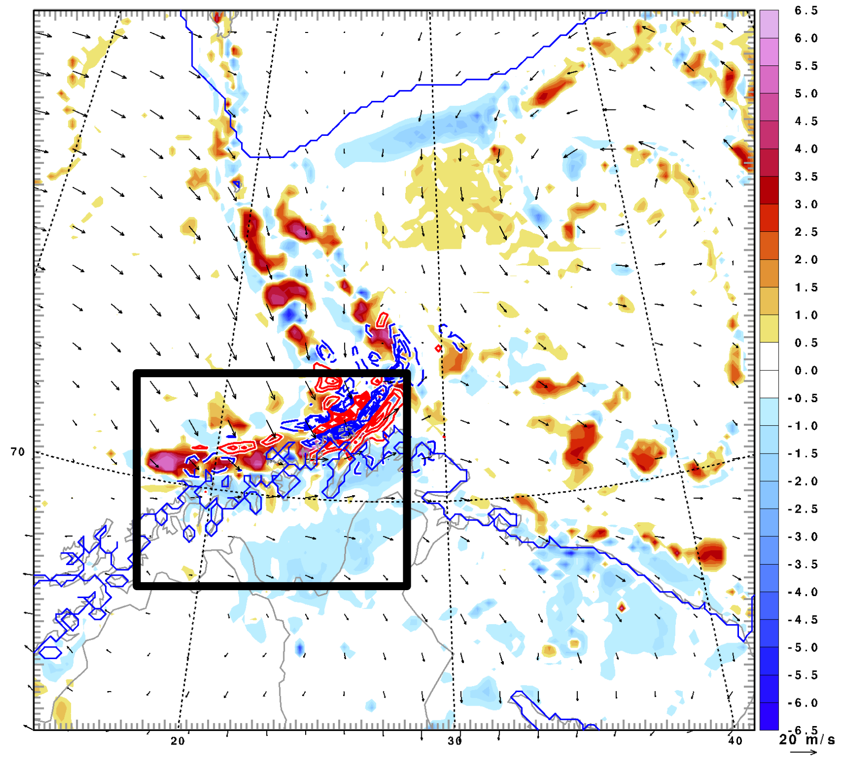

- Adjoint sensitivity based optimal perturbations evolved in the tangent linear and nonlinear models for 12h
- Changes in the polar low:
  - PV perturbation increase up to 8 PVU
  - Wind speed perturbation increase up to 21 m s^{-1}
  - Strong projection of the perturbations on to the diabatic heating rates near the polar low

TPV Intensity Adjoint Sensitivity

COAMPS (9 km) 12-h Forecast Sensitivity Valid at 0600 UTC 10 Feb 2011

Abs. vorticity ($x10^{-5}$ s^{-1}; shading), heights (black), rel. vorticity sensitivity (red/blue)

850-hPa

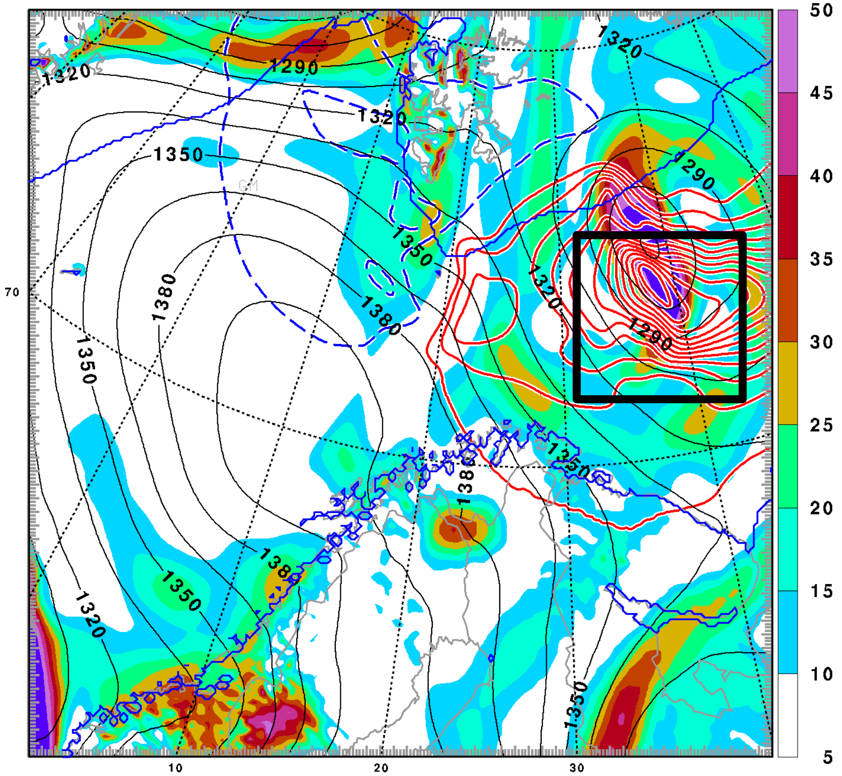

500-hPa

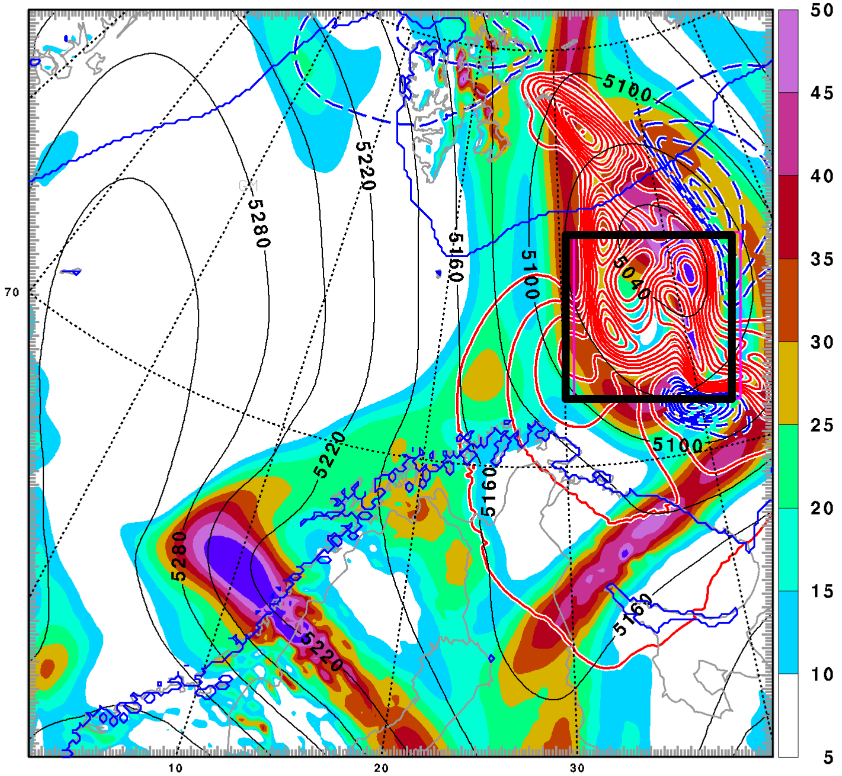

300-hPa

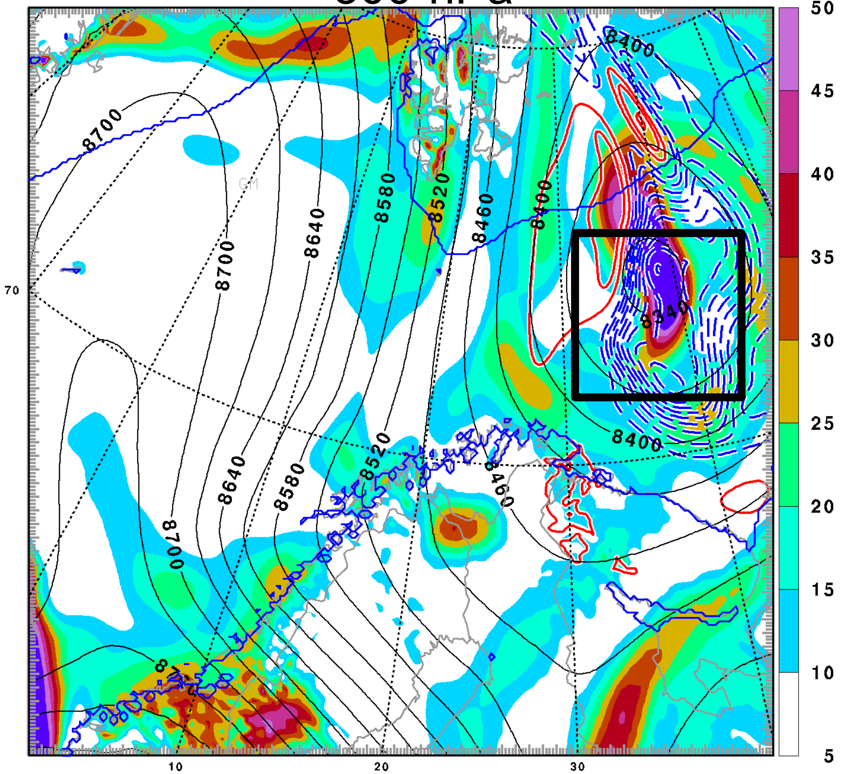

- PV response function is the 500-300 hPa PV over the forecast TPV at 12-h
- 12-h forecast relative vorticity associated with the TPV intensification is sensitive to:
  - Low- (850-hPa) and mid-(500-hPa) vorticity (and PV) in the TPV (↑0-h PV ⇨ ↑12-h PV in the TPV)
  - Upper level (300-hPa) vorticity (and PV) in the TPV (↓0-h PV ⇨ ↑12-h PV in the TPV)

U.S. NAVAL RESEARCH LABORATORY

TPV Adjoint Optimal Perturbations

COAMPS (9 km) 12-h Forecast and Optimal Perturbations Valid at 1800 UTC 10 Feb 2011

PV (PVU; shading), heights (black), PV optimal perturbations (PVU; red/blue)

925-hPa 500-hPa 300-hPa

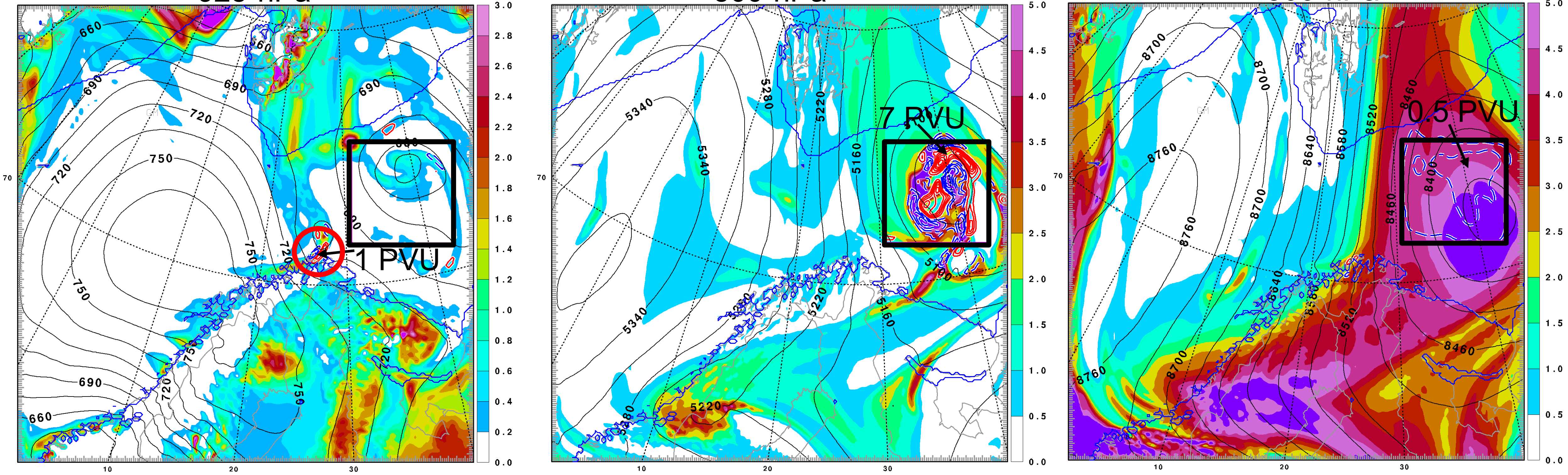

- Adjoint sensitivity based optimal perturbations evolved in the tangent linear and nonlinear models for 12h
- PV increases:
  - ➢ PV perturbations increase up to 7 PVU in the TPV in mid-levels, and a small PV decrease at 300-hPa
  - ➢ Small but focused region of PV increase of ~1 PVU near the polar low shear line

Adjoint Optimal Perturbations

Energy Budget

$$E = \frac{1}{2A}\int\left[(u'^2+v'^2+w'^2)+\frac{C_p}{T_r}T'^2+\frac{RT_r}{p^2_{sr}}p'^2+\frac{l_v^2}{C_pT_r}q_v'^2\right]dA\,d\sigma$$

Total KE PE IE Moist

- Adjoint based perturbations introduced at the initial time in the nonlinear model and evolved for 12h (polar low perturbations)
- Energy budget highlights the fast growth of the adjoint optimal perturbations
- Potential and moist energy (diabatic processes) contribute strongly to fast initial growth, with KE dominating by 12h
- Growth is more up-amplitude (relative to upscale) and growth is maximized at ~500-1000 km wavelengths.

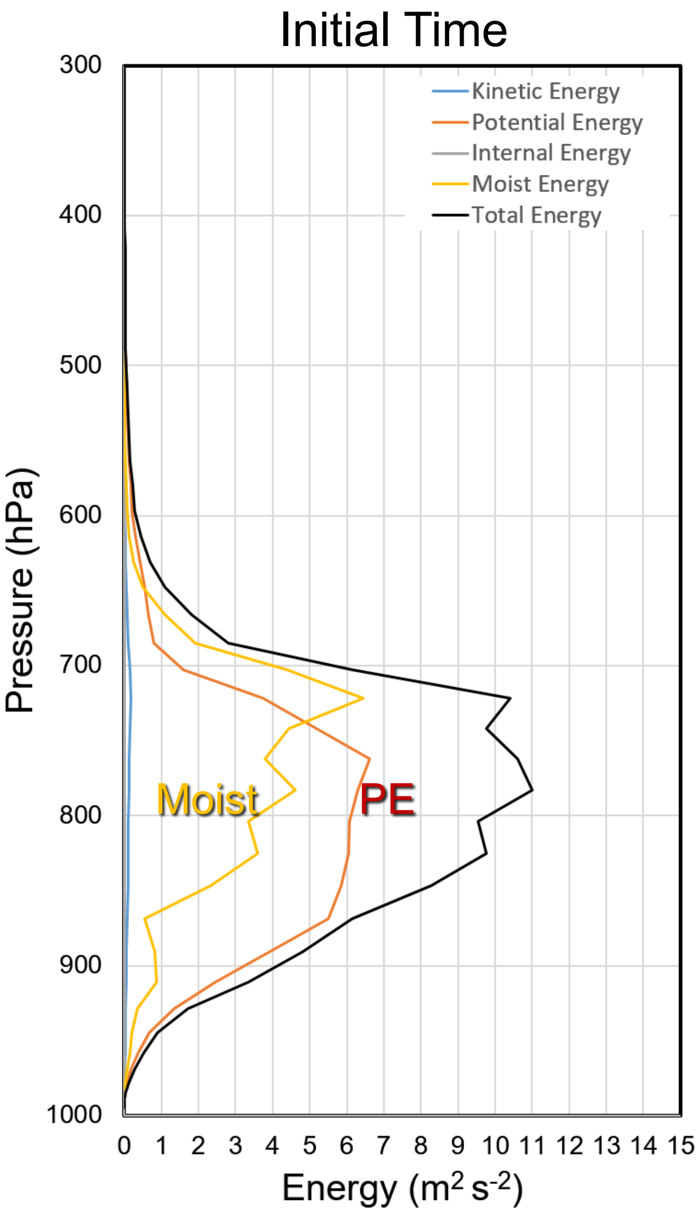

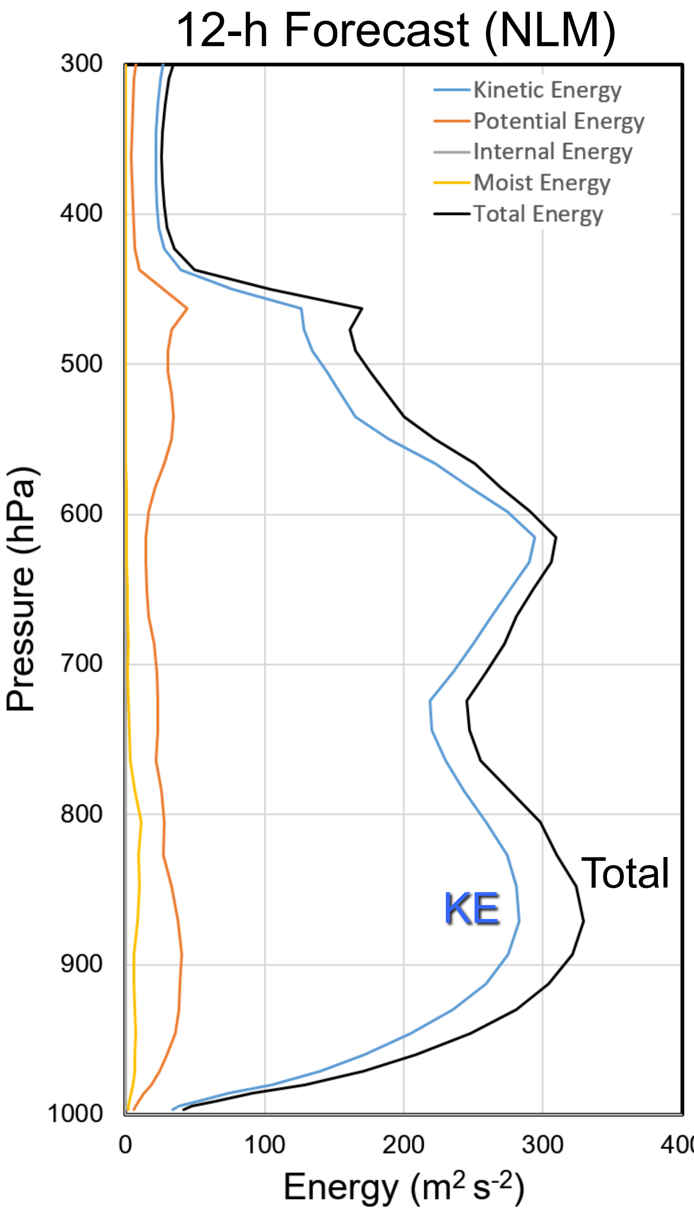

Summary

- **Low-level diabatic heating and TPVs lead to polar low rapid intensification:**
  - Climatologically, ~3/4 of polar lows are linked with TPVs (adjoint results are consistent)
  - Adjoint perturbations show rapid growth in the low-levels associated with strong moisture, vorticity, and air-sea flux sensitivities
- **Polar Low Predictability Barriers:**
  - Representations of diabatic processes; Limited moisture & wind observations in Arctic
  - Motivates the use of high-resolution ensembles
- **New Polar Low Observations in the Upcoming CAESAR Program (Feb.-Apr. 2024)**
  - CAESAR will focus on observations of shallow, precipitation clouds that form in cold-air outbreaks and polar lows over the open water using the NSF/NCAR C-130